

S15 Novel frontiers and challenges in magnetism **Nuevas fronteras y retos en magnetismo (CEMAG-IEEE Magnetics)**

11/07 Monday afternoon, Aula 1.12

- 15:00-15:05 Organisers
Presentation
- 15:05-15:50 Aurelien MANCHON (Aix-Marseille Université (AMU))
Exploring the Potentials of Spin-Orbitronics
- 15:50-16:10 Elvira Paz (INL)
Spintronic devices based on Magnetic Tunnel Junctions
- 16:10-16:20 Jorge Marqués Marchán (CSIC)
Distinguishing local demagnetization contribution to the magnetization process in multi-segmented nanowires
- 16:20-16:30 Santiago Osorio (CNEA)
Creation of single chiral soliton states in monoaxial helimagnets
- 16:30-16:40 Luis Sánchez-Tejerina San José (USAL)
Magnetic order excitation by magnetic fields from sub-picosecond structured laser pulses
- 16:40-16:50 Akashdeep Kamra (UAM)
Employing magnons for generating multi-qubit entangled states for quantum error correction
- 16:50-17:00 María Vélez Fraga (UNIOVI)
Bloch singularities and topological magnetic dipoles in a ferromagnetic microstructure
- 17:00-18:00 **Posters (IEEE Networking) and Coffee**
- 17:45-18:05 Saul Velez (UAM)
Chiral spintronics with magnetic insulators
- 18:05-18:15 Arantxa Fraile Rodríguez (UB)
Insights into the structural and magnetic texture of maghemite nanoflowers for biomedicine and environmental remediation
- 18:15-18:25 Rodrigo Martín Hernández (USAL)
Spatial isolation of femtosecond magnetic needles driven by azimuthally-polarized laser beams
- 18:25-18:35 Alonso José Campos Hernández (IMDEA Nanociencia)
FORC and coercivity angular measurements analysis of the magnetic interactions in arrays of FeNi nanowires
- 18:35-18:45 Aun Nawaz Khan (US)
Magnetocaloric effect in doped all-d-metal Ni-(Co)-Mn(X)-Ti (X = Fe and Cr) Heusler alloys
- 18:45-18:55 Ana Parente Campos (UCM)
Magnetic nanostructures with different spin textures and topological protection
- 18:55-19:05 Alejandro Sánchez Miñarro (ICMAB)
Spin-orbit mixed states in an electromagnetic field

19:05-19:15 Sebastian Bustingorry (CNEA)
Universal critical exponents of the magnetic domain wall depinning transition

Posters:

- 31** José Miguel García-Martín (CSIC)
Novel magnetic nanostructures: nanopillars and patterned antidots
- 32** Diego Caso Parajón (UAM)
Edge spin wave transmission through a vertex domain wall in triangular dots
- 33** Zaida Curbelo Cano (IMDEA Nanociencia)
Synthesizing MnAlC / hydrogel composites for 3D-printing of alternative permanent magnets
- 34** Jose Angel Fernandez Roldan (HZDR)
Current- and Oersted-field- dynamics of a Bloch Point in cylindrical Ni nanowires
- 35** Ester M. Palmero (IMDEA Nanociencia)
Role of the particle size in the development of customized permanent magnet composites and flexible filaments for additive manufacturing
- 36** Antonio David Subires Santana (DIPC)
Electronic band structure of the Co pnictide $\text{Ca}(\text{CoAs})_2$ probed by ARPES
- 37** Luis Moreno-Ramírez (US)
Temperature First Order Reversal Curves (TFORC) distributions of magnetocaloric materials
- 38** Miriam Jaafar (UAM)
Magnetic Force Microscopy for biomedical applications

Exploring the potentials of spin-orbitronics

Aurélien Manchon

Centre Interdisciplinaire de Nanoscience de Marseille (CINaM), Aix-Marseille University, France.

e-mail: aurelien.manchon@univ-amu.fr

The ever-increasing demand of information technology for power-efficient components has led to the search for alternative solutions to mainstream microelectronics. In this context, spintronics devices stand out as competitive candidates, especially for memory and logic applications. A promising route harvests unconventional transport properties arising from spin-orbit coupling in magnetic heterostructures lacking inversion symmetry.

In these systems, typically multilayers of transition-metal ferromagnets and heavy materials (e.g., W, Pt, Ta, Bi₂Se₃, WTe₂), interfacial spin-orbit coupling promotes a wealth of remarkable physical phenomena: the generation of spin-orbit torques, the interconversion between spin and charge currents, and the stabilization of topological magnetic skyrmions. These effects have gathered extraordinary interest and have led to remarkable experimental breakthroughs, including extremely fast magnetic reversal, terahertz emission, and current-driven skyrmion motion. The recent synthesis of novel classes of materials, including all-oxide heterostructures, noncollinear antiferromagnets, and van der Waals heterostructures, has profoundly enriched this vivid field of research by unlocking unforeseen forms of torques and magnetic interactions, thereby enhancing the functionalities of spin-orbitronic devices.

This lecture will provide a theoretical perspective of the advancement of the fascinating field of spin-orbitronics, focusing on two emblematic mechanisms: the spin-orbit torque and the Dzyaloshinskii-Moriya interaction. I will examine what theory and materials modeling can tell us about these two effects, and what future research directions they open. I will first introduce key concepts in spintronics, such as spin currents and spin-transfer torque, and show how spin-orbit coupling enables new physical effects of high interest for potential applications. I will present standard phenomenological descriptions of these two effects, spin-orbit torque and Dzyaloshinskii-Moriya interaction, determine the symmetry rules that govern them, and give a broad overview of the current state-of-the-art of the field from experimental and theoretical standpoints. Finally, I will explore how spin-orbitronics takes a completely new form in materials possessing low crystalline symmetries, such as Fe₃GeTe₂, CuPt/CoPt bilayers, and noncollinear antiferromagnets (e.g., Mn₃Sn).

I hope this seminar will not only encourage electrical engineers to engage in this beguiling field of research and explore the device implications of this new technology, but also reach out to scientists working in adjacent fields (terahertz science, for instance) who could bring inspiring new ideas to spintronics [1-5].

- [1] A. Manchon, J. Železný, I. M. Miron, T. Jungwirth, J. Sinova, A. Thiaville, K. Garello, and P. Gambardella, Current-induced spin-orbit torques in ferromagnetic and antiferromagnetic systems, *Rev. Mod. Phys.* **91**, 035004 (2019).
- [2] A. Belabbes, G. Bihlmayer, F. Bechstedt, S. Blügel, and A. Manchon, Hund's rule-driven Dzyaloshinskii-Moriya interaction at 3d-5d interfaces, *Phys. Rev. Lett.* **117**, 247202 (2016).
- [3] E. Jué, C. K. Safeer, M. Drouard, A. Lopez, P. Balint, L. Buda-Prejbeanu, O. Boulle, S. Auffret, A. Schuhl, A. Manchon, I. M. Miron, and G. Gaudin, Chiral damping of magnetic domain walls, *Nature Mater.* **15**, 272 (2016).
- [4] S. Laref, K.-W. Kim, and A. Manchon, Elusive Dzyaloshinskii-Moriya interaction in monolayer Fe₃GeTe₂, *Phys. Rev. B* **102**, 060402 (2020).
- [5] L. Liu et al., Symmetry-dependent field-free switching of perpendicular magnetization, *Nat. Nanotech.* **16**, 277 (2021).

Acknowledgements: This work was supported by the King Abdullah University of Science and Technology (KAUST, Thuwal, Saudi Arabia) and by the Excellence Initiative of Aix-Marseille Université - A*Midex, a French "Investissements d'Avenir" program.

Spintronic devices based on Magnetic Tunnel Junctions

Elvira Paz*, L. Benetti, T. Böhnert, A. Jenkins, A. Schulman, A. Talantsev, R. Ferreira

INL – International Iberian Nanotechnology Laboratory, Av. Mestre José Veiga s/n 4715-330 Braga, Portugal

*e-mail: elvira.paz@inl.int

Magnetic Tunnel Junction (MTJ) is a complex stack of different materials with a lot of different layers, where it is mandatory to have two ferromagnetic layers separated by a thin dielectric barrier and a mechanism to pin the polarization of one of the magnetic layers in a fixed direction, i.e., pinned layer. By tuning the thicknesses and materials of the different layers devices can be fabricated for a lot of different applications, in this presentation we are going to focus on magnetic sensors and spin-torque nano-oscillators (STNO).

Magnetic sensors have attracted significant interest having due to important applications in the automotive industry as rotation sensors and for the medical industry to measure the magnetic signals produced by our body. To achieve a large signal to noise ratio the sensing area should be as large as possible as the noise is inversely proportional to the area. To increase the area a lot of sensors can be connected in series, or the area of each sensor can be large. To have a linear variation of the resistance with the field the polarization of the pinned layer must be perpendicular to the easy axis of the other ferromagnetic layer, the free layer. The easy axis of the free layer can be set perpendicular by the shape anisotropy, by soft pinning the free layer [1,2] or by having an out of plane free layer.

With a soft pinned MTJ where 1102 pillars of $100 \times 100 \mu\text{m}^2$ are connected in series it is possible to detect down to $115 \text{ pT/Hz}^{0.5}$ at 196 Hz without amplification. These sensors were successfully integrated into commercial strain gauge devices, as a competitive alternative of extension-meters. Instead of direct measurement of extensions associated with a force, applied to a strain gauge, the MTJ sensor detects variations of magnetic field, associated with displacements of the magnet, mounted on the strain gauge platform. A resolution of positioning down to 100 nm is obtained without amplification.

When the dimensions of the MTJ pillars are reduced to the range of 100-400nm, new physical phenomena become noticeable, in particular spin transfer torque, that can be used to explore dynamic properties of the magnetization. Vortex nano-oscillators are a particular type of STNO which explore dynamics of free layers with a non-trivial and non-uniform micromagnetic configuration. These devices can generate RF currents, typically in the range of 100-1000MHz when excited with DC currents [3], and conversely, they can generate a DC output when excited with RF currents with frequencies matching the resonant states [4]. These devices have recently attracted a lot of attention due to their potential application in neuromorphic computation and the ongoing efforts will be reported.

The CMOS integration of these devices is very important for very dense devices, for example, sensors to perform magnetic imaging, an interesting application that these very sensitive sensors make possible, as shown in figure 1. In addition CMOS integration is essential for performing large scale computation with these devices (i.e., neuromorphic computing) where a lot of MTJs or a lot of connections are needed.

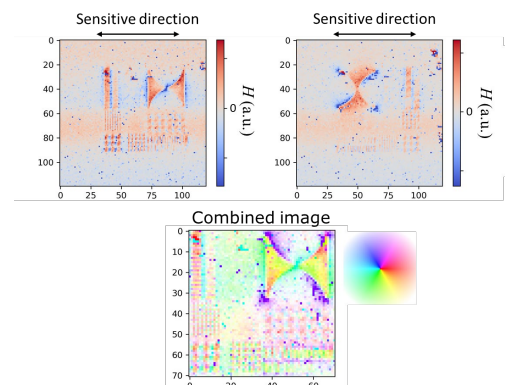


Figure 1. Magnetic image of a patterned multilayer [5nm Ta / 8nm NiFe] $\times 20$

- [1] E. Paz, S. Serrano-Guisan, R. Ferreira and P. P. Freitas, *Journal of Applied Physics* **115**, 17E501 (2014).
- [2] E. Paz, R. Ferreira and P. P. Freitas, *IEEE Transactions on Magnetics* **52**, 4002104 (2016).
- [3] J. D. Costa, S. Serrano-Guisan, B. Lacoste, A. S. Jenkins, T. Böhnert, M. Tarequzzaman, J. Borme, F. L. Deepak, E. Paz, J. Ventura, R. Ferreira and P. P. Freitas, *Scientific Reports* **7**, 7237 (2017).
- [4] A. Jenkins, L. San Emeterio Alvarez, S. Memshawy, P. Bortolotti, V. Cros, P. P. Freitas, R. Ferreira, *Communications Physics* **4**, 1-7 (2021).

Acknowledgements: FET-OPEN SpinAge, FET-Open RadioSpin, PT2020 Newwest.

Distinguishing local demagnetization contribution to the magnetization process in multisegmented nanowires

J. Marqués-Marchán^{1,*}, J.A. Fernandez-Roldan², C. Bran¹, R. Puttock^{3,4}, C. Barton³, J.A. Moreno⁵, J. Kösel^{6,7}, M. Vazquez¹, O. Kazakova³, O. Chubykalo-Fesenko¹, A. Asenjo¹

¹Instituto de Ciencia de Materiales de Madrid, CSIC, 28049 Madrid, Spain

²Helmholtz-Zentrum Dresden-Rossendorf e.V., Institute of Ion Beam Physics and Materials Research, 01328 Dresden, Germany

³National Physical Laboratory, Hampton Road, Teddington TW11 0LW, United Kingdom

⁴Department of Physics, Royal Holloway University of London, Egham TW20 0EX, United Kingdom

⁵Physical Science and Engineering Division, King Abdullah University of Science and Technology, Thuwal 239556900, Saudi Arabia

⁶Computer Electrical and Mathematical Science and Engineering Division, King Abdullah University of Science and Technology, Thuwal 23955-6900, Saudi Arabia

⁷Research Unit Sensor Applications, Sensor Systems Division, Silicon Austria Labs, A-9524 Villach, Austria

*e-mail: jorge.marques@csic.es

The excellent response of cylindrical magnetic nanowires (NWs) to external stimuli (magnetic, electrical or mechanical), as well as their interesting magnetic properties arising from their high aspect-ratio and curved geometry, position the NWs as promising materials for their use in different fields, ranging from biomedical to spintronics applications [1]. The versatility of these nanostructures is based on the tunability of their magnetic properties by the appropriate selection of the composition and morphology. For instance, the controlled reversal magnetization in cylindrical nanowires have proposed recently as an alternative to the three-dimensional (3D) racetrack memory devices [2]. Besides, the stochastic magnetization switching behaviour is attracting attention for the development of neuromorphic devices [3].

In this work, we present a study of the magnetization reversal process in multilayered CoNi/Cu nanowires. The non-standard MFM images obtained under in-plane magnetic field, so called 3D images [4], are correlated with the magnetoresistance measurements and micromagnetic simulations. Figure 1 shows an MFM 3D image of the NW. Thanks to this combined studied, the contribution of the individual segments to the demagnetization process can be distinguished. Results show that the magnetization reversal process in these nanowires does not occur through a single Barkhausen jump, but by several switching corresponding to the magnetization reversal processes of individual CoNi segments in the NW. Moreover, the existence of vortex states is confirmed by their footprint in the magnetoresistance measurements as well as in the magnetic imaging measurements. In addition, the either deterministic or stochastic character of the magnetization process is analysed. We observe different switching fields among the segments due to a slightly variation in geometrical parameters or magnetic anisotropy.

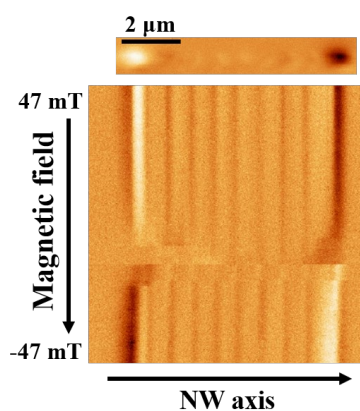


Figure 1. Standard MFM image (up) and 3D image (below) of a CoNi/Cu NW.

[1] Moreno, J.A.; Bran, C.; Vazquez, M.; Kosel, J., *IEEE Transactions on Magnetics* **57** (2021).

[2] Rial, J.; Proenca, M.P., *Nanomaterials* **10**, 1-14 (2020).

[3] Azam, M.A. et al., *Nanotechnology* **31**(14), 145201 (2020).

[4] Jaafar, M. et al., *Nanoscale Res. Lett.* **6**(1), 407 (2011).

Creation of single chiral soliton states in monoaxial helimagnets

Santiago A. Osorio^{1,*}, Victor Laliena², Javier Campo³, Sebastian Bustingorry¹

¹*Instituto de Nanociencia y Nanotecnología, CNEA-CONICET, Centro Atómico Bariloche, (R8402AGP) S. C. de Bariloche, Río Negro, Argentina.* ²*Department of Applied Mathematics, University of Zaragoza, C/María de Luna, 3, 50018 Zaragoza, Spain.* ³*Aragon Nanoscience and Materials Institute (CSIC-University of Zaragoza) and Condensed Matter Physics Department, University of Zaragoza, C/Pedro Cerbuna 12, 50009 Zaragoza, Spain.*

*e-mail: santiago.osorio@cab.cnea.gov.ar

In monoaxial chiral helimagnets the Dzyaloshinskii-Moriya interaction favors inhomogeneous distributions of the magnetization with chiral modulations termed chiral solitons. These localized magnetization textures crystallize at low magnetic field leading to the emergence of a chiral soliton lattice [1]. In a magnetic field perpendicular to the chiral axis the system undergoes a phase transition to the uniform state at a critical field B_c [2]. Above this critical field value, a single chiral soliton comprises the lowest level excitation over the stable uniform state, surviving as a metastable configuration [3]. We study theoretically, using micromagnetic simulations, the metastability of a single chiral soliton and propose a strategy to obtain such a state from the chiral soliton lattice [4]. We show that using spin-polarized currents chiral solitons in the chiral soliton lattice can be pushed against each other and it is possible to destroy the solitons one-by-one in a controlled way. A state with one chiral soliton can be obtained by these means for a suitable choice of the external field and the current density (Fig. 1). An important feature of our proposal is that it exhibits a strong robustness against the magnetization distribution in the initial state, even if the initial state is metastable. Our proposal could be relevant in the study of metastable solitons from both the experimental and technological applications.

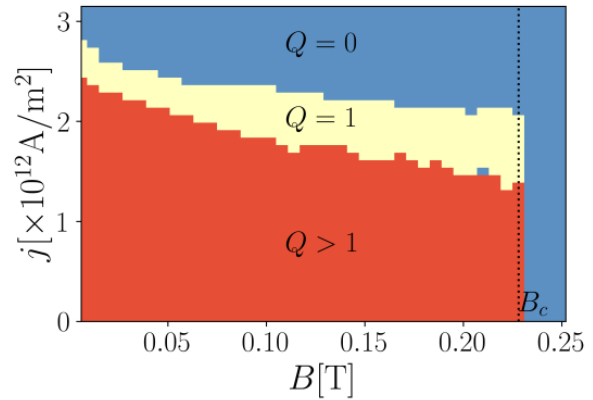


Figure 1. Phase diagram in the $j - B$ space, with j the applied current density and B the external magnetic field, indicating the final number of chiral solitons Q after applying a pulse of current. In the yellow region a metastable single chiral soliton is obtained ($Q = 1$).

[1] Y. Togawa, Y. Kousaka, K. Inoue and J. Kishine, *J. Phys. Soc. Jpn.* **85**, 112001 (2016).

[2] V. Laliena *et al*, *Phys. Rev. B* **93**, 134424 (2016).

[3] V. Laliena, S. Bustingorry, and J. Campo, *Sci. Rep.* **10**, 20430 (2020).

[4] S. A. Osorio, V. Laliena, J. Campo and S. Bustingorry, *Appl. Phys. Lett.* **119**, 222405 (2021).

Acknowledgements: This work was supported by Grant No. PGC2018099024B100 funded by MCIN/AEI/10.13039/501100011033. Grants OTR02223 from CSIC/MICIN and DGA-M4 from Diputación General de Aragón, Spain, are also acknowledged. This work was also supported by the Grant No. PICT 2017-0906 from the Agencia Nacional de Promoción Científica y Tecnológica, Argentina.

Magnetic order excitation by magnetic fields from sub-picosecond structured laser pulses

Luis Sánchez-Tejerina^{1,*}, Rodrigo Martín-Hernández¹, Rocío Yanes², Luis Plaja¹, Luis López-Díaz², Carlos Hernández-García¹

¹Grupo de Investigación en Aplicaciones del Láser y Fotónica, Dpto. Física Aplicada, Universidad de Salamanca, E-37008, Salamanca, Spain. ²Dpto. Física Aplicada, Universidad de Salamanca, E-37008, Salamanca, Spain.

*e-mail: luis.stsj@usal.es

The manipulation of magnetic properties can be exploited in a wide range of applications, such as detectors, actuators, memories, etc. Ultrafast, yet efficient, ways of manipulating magnetic textures could widen even more the use of magnetically ordered systems. The pioneering work on ultrafast laser induced demagnetization in Ni [1], demonstrated that ultrafast laser sources can promote femtosecond (fs) ferromagnetic switching, opening the door to a large number of theoretical and experimental studies on femtomagnetism. Recent technological advances in structured laser sources are opening the door to novel magnetic manipulation schemes. In particular, it has been recently proposed that Tesla-scale fs magnetic fields, isolated from the electric field, can be obtained through the use of ultrafast azimuthally polarized laser beams [2]. Such configuration offers the opportunity to perform pure magnetic interactions with an intense fs B field.

In the present work [3] we show that non-linear magnetic field effects driven by structured laser pulses provide a way to manipulate the magnetic order of ferro- and antiferromagnetic materials. We introduce a novel ferromagnetic switching scheme on sub-ps time-scales by purely magnetic precession of the magnetization with field amplitudes of hundreds of Tesla. We provide an analytical expression that relates the magnetic field amplitude, frequency and pulse duration to achieve switching. Interestingly, lower magnetic fields are enough to excite self-oscillations in AFM materials even after the laser pulse. In this case, the effect can be enhanced or inhibited by the application of a train of laser pulses by properly choosing the polarization and time delay between the pulses. In this sense, it could be possible to construct an artificial neuron excited by this mechanism. The isolation of the magnetic field avoids the heating due to the electric field which may drive stochastic processes or even damage the sample. Our work opens a promising scenario for the manipulation of magnetic states on fs time scales through the use of structured laser beams.

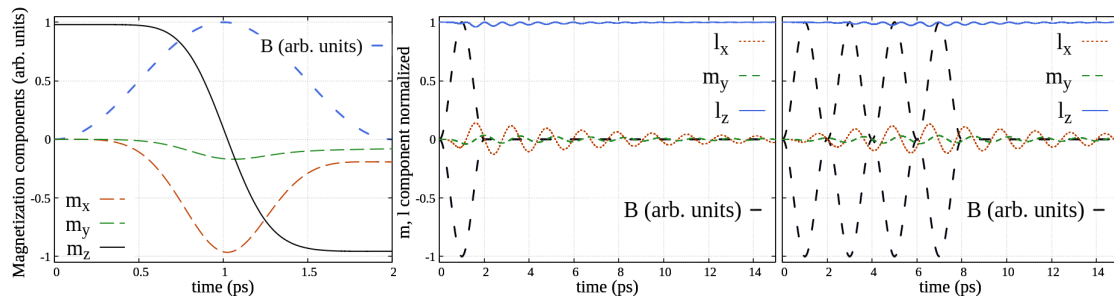


Figure 1. (a) Ferromagnetic switching due to a laser pulse with amplitude $B = 400$ T, main frequency $f = 100$ THz and pulse width $t_p = 750$ fs. (b) Antiferromagnetic oscillations after a laser pulse with amplitude $B = 200$ T, main frequency $f = 125$ THz and pulse width $t_p = 637.5$ fs. (c) Antiferromagnetic oscillations after four laser pulses with amplitude $B = 120$ T, main frequency $f = 125$ THz and pulse width $t_p = 637.5$ fs. The amplitude of the oscillations is the same as in (b).

[1] E. Beaurepaire, J.-C. Merle, A. Daunois, and J.-Y. Bigot, *Phys. Rev. Lett.* **76**, 4250 (1996).

[2] M. Blanco, F. Cambronero, M. T. Flores-Arias, E. Conejero Jarque, L. Plaja, and C. Hernández-García *ACS Photonics* **6** (2019).

[3] L. Sánchez-Tejerina, R. Yanes, R. Martín-Hernández, L. Plaja, L. López-Díaz, C. Hernández-García, in preparation.

Acknowledgements: This work has been funded by the ERC Starting Grant ATTOSTRUCTURA, grant agreement No. 851201; Ministerio de Ciencia de Innovación y Universidades (PID2019-106910GB-I00, RYC-2017-22745); Junta de Castilla y León FEDER (SA287P18).

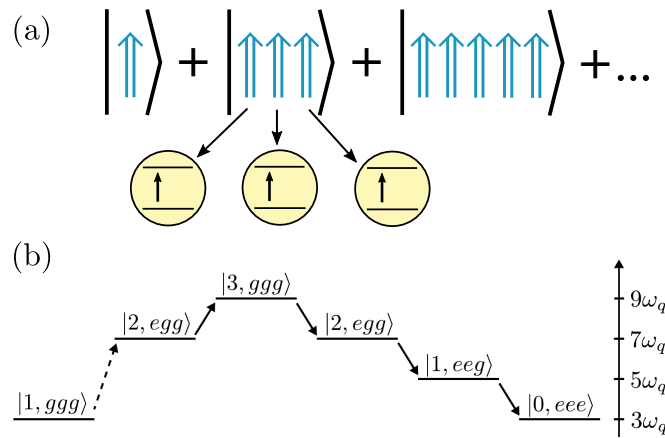
Employing magnons for generating multi-qubit entangled states for quantum error correction

Ida C. Skogvoll¹, Jonas Lidal¹, Jeroen Danon¹, and Akashdeep Kamra^{2,1,*}

¹Center for Quantum Spintronics, Department of Physics, Norwegian University of Science and Technology, Trondheim NO-7491, Norway. ²Condensed Matter Physics Center (IFIMAC) and Departamento de Física Teórica de la Materia Condensada, Universidad Autónoma de Madrid, Madrid E-28049, Spain.

*e-mail: akashdeep.kamra@uam.es

The ongoing rapid progress towards quantum technologies relies on and strives for new hybrid platforms optimized for specific quantum computation and communication tasks. We theoretically study a spin qubit exchange-coupled to an anisotropic ferromagnet that hosts magnons with a controllable degree of intrinsic squeezing. We find this system to physically realize the quantum Rabi model from isotropic to the Jaynes-Cummings limit with coupling strengths that can foray into the deep-strong regime. We demonstrate that the composite nature of the squeezed-magnon enables concurrent excitation of 3 spin qubits coupled to the same magnet. Thus, 3-qubit Greenberger-Horne-Zeilinger and related states needed for implementing Shor's quantum error correction code can be robustly generated. Our analysis highlights some unique advantages offered by this hybrid platform and hopes to motivate corresponding experimental efforts.



[1] I. C. Skogvoll, J. Lidal, J. Danon, and A. Kamra, *Phys. Rev. Applied* **16**, 064008 (2021).

Acknowledgements: We acknowledge financial support from the Research Council of Norway through its Centers of Excellence funding scheme, project 262633, “QuSpin”, and the Spanish Ministry for Science and Innovation – AEI Grant CEX2018-000805-M (through the “Maria de Maeztu” Programme for Units of Excellence in R&D).

Bloch singularities and topological magnetic dipoles in a ferromagnetic microstructure

Javier Hermosa^{1,2}, Aurelio Hierro-Rodríguez^{1,2}, Carlos Quirós^{1,2}, José I. Martín^{1,2}, Andrea Sorrentino³, Lucía Aballe³, Eva Pereiro³, **María Vélez**^{1,2,*}, Salvador Ferrer³

¹Depto. Física, Universidad de Oviedo, 33007 Oviedo, Spain. ²CINN (CSIC – Universidad de Oviedo), 33940 El Entrego, Spain. ³ALBA Synchrotron, 08290 Cerdanyola del Vallès, Spain.

*e-mail: mvelez@uniovi.es

Bloch points are magnetic singularities defined by the condition of zero magnetization ($m_x = m_y = m_z = 0$). They are essential for the understanding of magnetization reversal in many different systems such as stripe domain patterns, skyrmion lattices or magnetic nanowires. The singular character of Bloch points is associated with a topological charge defined by the flux of an emergent field \mathbf{B}^e across a closed surface $Q = \frac{1}{4\pi\hbar} \oint \mathbf{B}^e \cdot d\mathbf{S}$ [1] with $B_i^e = \frac{\hbar}{2} \epsilon_{ijk} \mathbf{m} \cdot \partial_j \mathbf{m} \times \partial_k \mathbf{m}$. The quantitative analysis of these singularities requires experimental vector magnetization maps $\mathbf{m}(\mathbf{r})$ with high spatial resolution, which is possible by means of X-ray vector magnetic tomography [2].

We present high resolution vector magnetic tomograms of 140 nm thick permalloy microstructures fabricated by e-beam lithography on a Si-N membrane [3], obtained at the Mistral Beamline of the ALBA Synchrotron. Among the magnetic singularities found are the Bloch point topological dipole shown in Figure 1: Two closely spaced Bloch points are identified consisting of a CW vortex and either a head-to-head domain wall (at BP(-Q)) or a tail-to-tail domain wall (at BP(+Q)). The Bloch points mediate the chirality transitions that occur at the kinks of the central domain wall in the microstructure. The calculated emergent field lines tend to aggregate into bundles carrying a fractional amount of the emergent field flux of each individual Bloch point, which can be used to generalize the concept of magnetic vortex in low symmetry configurations without a well-defined polarity and chirality.

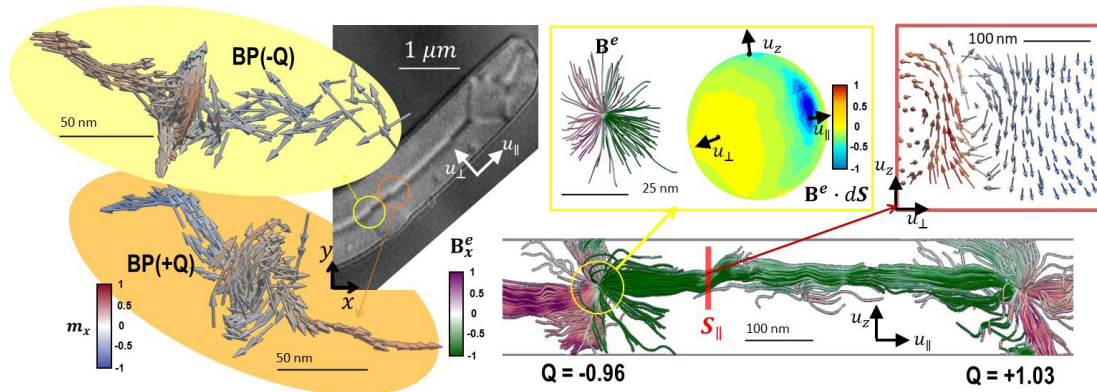


Figure 1. Magnetization configuration $\mathbf{m}(\mathbf{r})$ at a Bloch point dipole with opposite topological charges reconstructed by X-ray vector magnetic tomography. Bloch points decorate the kinks of the central domain wall of the permalloy microstructure (yellow and orange circles in the X-ray magnetic transmission microscopy image at normal incidence). The emergent field lines \mathbf{B}^e (calculated from the experimental $\mathbf{m}(\mathbf{r})$) deviate strongly from the spherical symmetry of an isolated monopole, as shown by the hot spots of emergent field flux $\mathbf{B}^e \cdot d\mathbf{S}$ on a spherical shell surrounding BP(-Q). A cross section of the magnetic configuration at a bundle of \mathbf{B}^e lines shows that it corresponds to an asymmetric vortex across the sample thickness.

[1] B. Göbel, I. Mertig, O. A. Tretiakov, *Physics Reports* **895**, 1-28 (2021)

[2] A. Hierro-Rodríguez, C. Quirós, A. Sorrentino, L. M. Alvarez-Prado, J. I. Martín, J. M. Alameda, S. McVitie, E. Pereiro, M. Vélez & S. Ferrer, *Nature Comm.* **11**, 6382 (2020).

[3] J. Hermosa, A. Hierro-Rodríguez, C. Quirós, M. Vélez, A. Sorrentino, L. Aballe, E. Pereiro, S. Ferrer and J. I. Martín, *Micromachines* **13**, 204 (2022).

Acknowledgements: Work supported by Spanish MICINN grant PID2019-104604RB/AEI/10.13039/501100011033 and by Asturias FICYT, grant AYUD/2021/51185 with the support of FEDER funds.

Chiral spintronics with magnetic insulators

Saül Vélez

Departamento de Física de la Materia Condensada & IFIMAC, Universidad Autónoma de Madrid, Spain.

e-mail: saul.velez@uam.es

The use of the spin of the electrons in devices is having a tremendous impact on our electronics and computing technologies. Tell-tale examples are found in the electric switching and reading of magnetic tunnel junctions as well as in the controlled displacement of magnetic domain walls in magnetic thin films. Despite the enormous progress that has been made, current devices are restricted to the use of metallic ferromagnets, which typically suffer from high losses and are limited in frequency.

Magnetic insulators (MIs), such as rare earth garnets ($R_3\text{Fe}_5\text{O}_{12}$; $R=\text{Y, Tm, ...}$), have attracted a lot of interest because of their low Gilbert damping and high-frequency dynamics. Although being electrically insulating, MIs can couple to spin currents, making thus possible to employ these materials as active elements in electronic devices.

In this talk, we will show how we can stabilize chiral domain walls and skyrmions in $\text{Tm}_3\text{Fe}_5\text{O}_{12}$ (TmIG) coupled to Pt and manipulate them by proximity electric currents (Fig. 1) [1,2]. We will demonstrate the chiral nature of the domain walls and skyrmions via nitrogen-vacancy magnetometry and investigate their dynamics driven by current pulses. Our results reveal that the domain walls in TmIG exhibit mobilities comparable to those achieved with metallic ferromagnets and show that the dynamics of the skyrmions are governed by the ferrimagnetic order of the crystal and pinning, resulting in a large skyrmion Hall effect characterized by a negative deflection angle and hopping motion. Further, we will show that the mobility of the walls and skyrmions can be modified by coupling TmIG to an in-plane magnetized $\text{Y}_3\text{Fe}_5\text{O}_{12}$ (YIG) layer, which distorts the spin texture of the domain walls and skyrmions leading to a directional-dependent rectification of their dynamics. This effect, which is equivalent to a magnetic ratchet, is exploited to control the flow of domain walls and skyrmions in devices. Finally, we will demonstrate that chiral interactions in YIG leads to a magnetic-field dependent directional propagation of spin waves, an effect analogous to drift currents driven by electric fields in conductors [3].

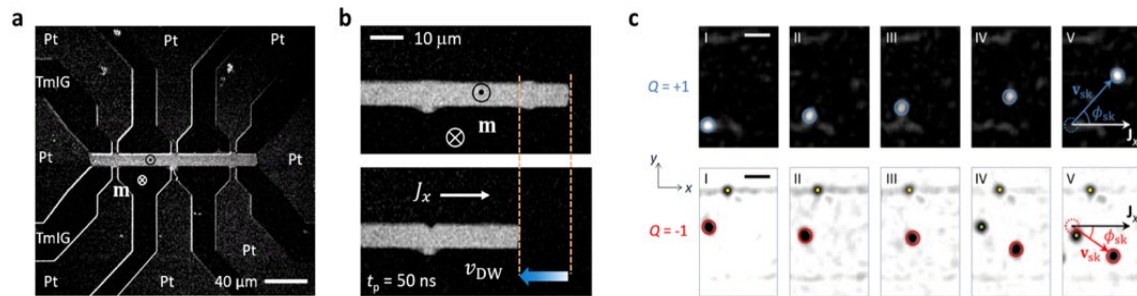


Figure 1. (a) Magneto-optical Kerr effect (MOKE) image of a TmIG/Pt device showing current-induced switching of TmIG (bright region). (b) Demonstration of current-driven wall motion. A current pulse $J_x \sim 10^{12}$ A m⁻² in Pt drives the walls in TmIG at velocities v_{DW} of 300 m/s. (c) MOKE images showing the displacement of skyrmions in YIG/TmIG/Pt following a sequence of current pulses. The topological charge of the skyrmions (Q), which can be controlled by the orientation of the skyrmion core (bright/dark), results in a transverse deflection of the skyrmions.

[1] S. Vélez et al., *Nat. Comm.* **10**, 4750 (2019).

[2] S. Vélez et al., *Nat. Nanotech.* (2022).

[3] R. Schlitz et al., *Phys. Rev. Lett.* **126**, 257201 (2021).

Insights into the structural and magnetic texture of maghemite nanoflowers for biomedicine and environmental remediation

M. Escoda-Torroella^{1,2,*}, C. Moya¹⁻³, A. Fraile Rodríguez^{1,2,*}, A. Gallo-Cordova⁴, M.P. Morales⁴,
A. Labarta^{1,2}, X. Batlle^{1,2}

¹Departament de Física de la Matèria Condensada, Martí i Franquès 1, 08028 Barcelona, Spain. ²Institut de Nanociència i Nanotecnologia (IN2UB), Universitat de Barcelona, 08028 Barcelona, Spain.

³Université libre de Bruxelles, Engineering of Molecular Nanosystems, 1050 Bruxelles, Belgium. ⁴Instituto de Ciencia de Materiales de Madrid, ICMM/CSIC, 28049 Madrid, Spain.

*e-mail: arantxa.fraile@ub.edu

Single-core magnetite/maghemite nanoparticles have been extensively studied because of their outstanding properties for biomedical and environmental applications [1,2]. Recently, great interest has focused on multicore nanoparticles, such as aggregates of cores arranged as nanoflower (NF)-like structures. Nevertheless, there is still a lot to understand about both the structure and magnetic properties of the NF to achieve good control over their performance in applications. In particular, the origin of the nearly demagnetized remanent state has still to be interpreted. In this work, three different samples synthesized by the polyol method were studied [3,4]. The size of the NFs (i.e., the overall size of the aggregate) was determined by transmission electron microscopy (TEM), obtaining values of 38 ± 10 nm, 122 ± 14 nm, and 379 ± 135 nm for NF40, NF100, and NF400 samples, respectively. All the samples showed an individual core size of ca. 5 nm, which was determined by TEM. Nevertheless, the crystalline size obtained by X-ray diffraction was about twice the size of the individual cores measured by TEM, showing a crystallographic correlation length that extended well beyond the individual cores. In addition, selected area electron diffraction patterns were not the ones expected for a polycrystalline sample as they showed a high degree of texture associated with preferential orientations of the cores within the NF. This complex crystalline structure led to hysteresis loops showing high values of both saturation magnetization (ca. 80 emu/g) and initial susceptibility, but with almost zero remanent magnetization and coercive field at 300 K. Therefore, a deeper understanding of the internal magnetic structure of the NF and the corresponding magnetic properties are key to optimize their performance in applications.

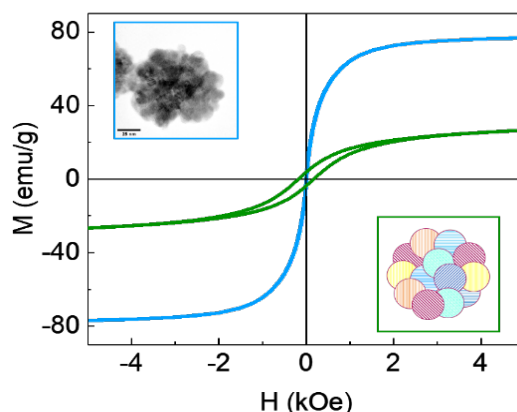


Figure 1. Comparison of the hysteresis cycles of a polycrystalline nanoparticle (green) and a NF (blue).

- [1] X. Batlle and A. Labarta, *J. Phys. D. Appl. Phys.* **35**, R152 (2002).
- [2] X. Batlle, *et al.*, *J. Magn. Magn. Mater.* **543**, 168594 (2022).
- [3] Gavián, H. *et al.*, *Part. Part. Syst. Charact.* **34**, 1–12 (2017).
- [4] M. Escoda-Torroella, 2022, Tuning the performance of magnetic, semiconductor, and multifunctional hybrid nanostructures, Doctoral Thesis, Universitat de Barcelona, Barcelona.

Acknowledgements: The work was supported by Spanish MCIU and AEI (MAT2015-68772-P; PGC2018-097789-B-I00) and European Union FEDER funds. M.E-T. acknowledges Spanish MCIU for BES-2016-077527.

Spatial isolation of femtosecond magnetic needles driven by azimuthally-polarized laser beams

Rodrigo Martín-Hernández*, Luis Sánchez-Tejerina, Enrique Conejero Jarque,
Luis Plaja, Carlos Hernández-García

Grupo de Investigación en Aplicaciones del Láser y Fotónica, Departamento de Física Aplicada, Universidad de Salamanca, E-37008, Salamanca, Spain.

*e-mail: rodrigomh@usal.es

Femtosecond laser sources have great potential to trigger, control, and observe ultrafast magnetic phenomena. Since the pioneering work on ultrafast laser-induced demagnetization by Beaupaire et al. [1], the interest on the potential applications of ultrafast laser pulses in magnetism has boosted. In particular, the development of ultrafast structured light beams has opened new perspectives in the field. Recently, it has been shown how Tesla-scale femtosecond magnetic fields, isolated from the electric field in a spatial volume, can be obtained from the interaction between azimuthally polarized vector beams and metallic nanoantennas [2]. These ultrafast isolated magnetic sources have opened a new perspective in ultrafast magnetism to study pure magnetic interactions where the key role is played by the magnetic, like magnetic switching in ferromagnetic materials [3] or oscillations in the Néel vector in antiferromagnetic materials.

In this work, we study the effect of different antenna geometries to optimize the efficiency and isolation of ultrafast magnetic fields. We have performed simulations using the Particle-In-Cell code OSIRIS [4], where circular apertured antennas generate isolated magnetic nanoprobes (fig. 1 a). However, a significant magnetic-to-electric field ratio is limited to distanced of few nanometers. Our simulations demonstrate how novel geometries enhance this contrast, allowing to keep the electric field below the sample damage threshold. As an example, the use of a double apertured antenna (Fig. 1 b), enhances the contrast ratio by a factor of three (Fig. 1 c). Further optimization of the antenna geometry could boost this contrast enhancement. Our work paves the route to employ polarization structured laser beams along metallic nanoantennas to achieve pure magnetic interactions with matter at ultrafast scales.

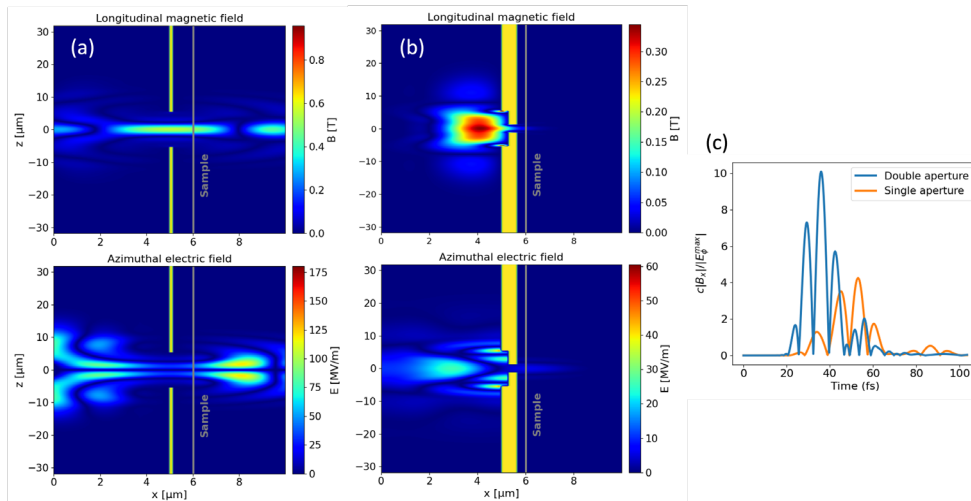


Figure 1: Spatial distribution, at $y=0$, of the longitudinal magnetic and azimuthal electric fields using (a) a single apertured antenna, as proposed in [2], and (b), a double apertured antenna. (c) Temporal evolution of the contrast at the sample for both antennas. The driving laser is a two-period $5 \mu\text{m}$ pulse, with a peak amplitude of 151 MV/m .

[1] E. Beaupaire, J.-C. Merle, et al., *Phys. Rev. Lett.* **76**, 4250 (1996).

[2] M. Blanco, F. Cambrero, M. T. Flores-Arias, E. Conejero Jarque, et al., *ACS Photonics* **6**, 38 (2019).

[3] L. Sánchez-Tejerina, R. Yanes, R. Martín-Hernández, L. Plaja, L. López-Díaz, C. Hernández-García, *in preparation*.

[4] R. A. Fonseca, L. O. Silva, F. S. Tung, et al., *Lecture Notes in Computer Science* **2331**, 342 (2002).

Acknowledgements: European Research Council (851201); Ministerio de Ciencia de Innovación y Universidades (PID2019-106910GB-I00, RYC-2017-22745); Junta de Castilla y León FEDER (SA287P18).

FORC and coercivity angular measurements analysis of the magnetic interactions in arrays of FeNi nanowires

Alonso J. Campos-Hernandez*, Ester M. Palmero, Alberto Bollero

Group of Permanent Magnets and Applications, IMDEA Nanociencia, 28049, Madrid, Spain.

*e-mail: alonsojose.campos@imdea.org

Compositional variation in magnetic nanowires (NWs) permits the tailoring of the magnetic properties under controlled synthesis conditions [1]. In this study arrays of FeNi NWs have been electrodeposited into anodized aluminum oxide (AAO) membranes (Fig. 1a). Chemical composition analysis of the samples showed anomalous co-deposition, where Fe deposits in ratios higher than its electrolyte molar fraction under different trends. The trends observed within this behaviour were explained within a modified Bocris-Drazic-Despic (BDD) model [2].

Coercivities (H_c) ranging from 0.2 kOe to 1.0 kOe were obtained (Fig. 1b), observing an increase in H_c for a diminished Fe concentration. The angular study of the magnetization reversal mechanisms (dominated by a transverse domain wall mechanism) hinted at the decrease in the magnetostatic interactions between NWs as the source of the rise in H_c . First-order reversal curve (FORC) analysis indicated a reduced value of the magnetic interactions in the arrays, except for the $\text{Fe}_{0.80}\text{Ni}_{0.20}$ NWs which showed a FORC diagram corresponding to magnetically interacting NWs (Fig. 1c). All the diagrams showed a high-intensity spot at around $H_c = 1$ kOe, with weakening intensity for an increased Fe content due to the higher interactions.

This work shows the possibility of tailoring the magnetic properties of FeNi NWs by tuning the electrochemical parameters and, thus, their composition and crystallographic structure. This approach is of interest in developing NW-based applications such as magnetic recording and sensing devices, and opens the path to explore the possibility of forming ordered phases with outstanding permanent magnet properties (e.g., the L_{10} -ordered FeNi phase [3]).

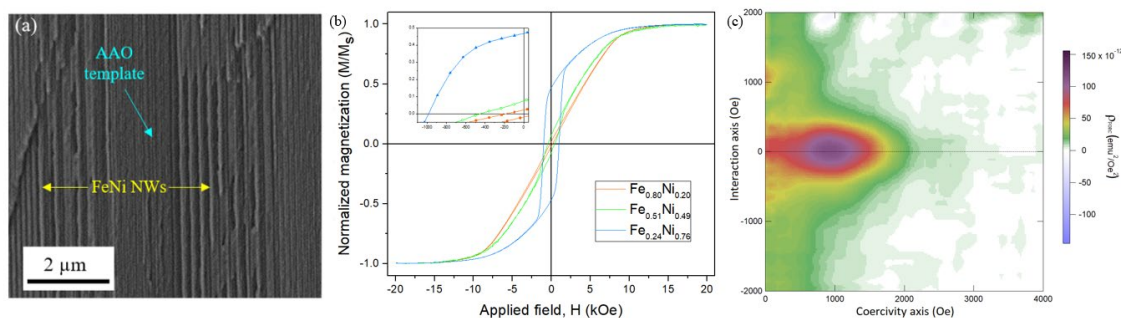


Figure 1. (a) SEM image of an array of FeNi NWs into an AAO membrane; (b) room temperature hysteresis loops measured for arrays of FeNi NWs with different compositions; and (c) FORC diagram for $\text{Fe}_{0.80}\text{Ni}_{0.20}$ NWs.

[1] Palmero, E. M. *et al.*, *J. Appl. Phys.* **116**, 033908 (2014).

[2] Dragos O. *et al.*, *J. Electrochem. Soc.* **163**, 83-94 (2015).

[3] Lewis, L. H. *et al.*, *J. Phys.: Condens. Matter* **26**, 064213 (2014).

Acknowledgements: Authors acknowledge financial support from EU M-ERA.NET and MICINN through the projects *COSMAG* (PCI2020-112143) and *NEXUS* (PID2020-11521RB-C21). A.J.C.-H. acknowledges support from “La Caixa” Foundation (ID 100010434) through the Doctoral INPhINIT Incoming program (LCF/BQ/DI20/1178002). E.M.P. acknowledges support from AEI through the Juan de la Cierva – Incorporación program (IJC2020-043011-I/MCIN/AEI/10.13039/501100011033) and EU by NextGenerationEU/PRTR.

Magnetocaloric effect in doped all-d-metal Ni-(Co)-Mn(X)-Ti (X = Fe and Cr) Heusler alloys

Aun N. Khan*, Luis M. Moreno-Ramírez, Álvaro Díaz-García, Jia Yan Law, Victorino Franco

Dpto. Física de la Materia Condensada. ICMS-CSIC. Universidad de Sevilla, P.O. Box 1065, Sevilla 41080, Spain.

*e-mail: akhan@us.es

All-d-metal Heusler alloys show elevated magnetocaloric/barocaloric effects ascribed to the undergoing martensitic transformation while retaining excellent mechanical properties in contrast to other well studied Heusler alloys [1,2]. However, for magnetocaloric applications of this system, high magnetic fields are still needed (much larger than those expected in real applications around 1-2 T) to obtain significant values and to overcome the hysteresis ascribed to the transformation and, therefore, for being considered as a potential candidate for magnetic refrigeration systems. In this work, we synthesized by arc melting a series of doped all-d-metal Ni-(Co)-Mn(X)-Ti (X = Fe and Cr) Heusler alloys (with parent composition of $\text{Ni}_{36}\text{Co}_{14}\text{Mn}_{35}\text{Ti}_{15}$) and investigate its martensitic transformations and magnetocaloric properties. On the one hand, doping the alloy with Cr (1 and 3 at.%) increases latent heat due to the increase of the martensite cell distortion but also leads to the overlapping of the martensitic and Curie transitions (increases the martensitic transition temperature and reduces the Curie temperature) which significantly reduces the magnetization difference between austenite and martensite and, therefore, reducing significantly the isothermal entropy change with respect to the parent alloy. Both combined effects drastically reduce the magnetocaloric performance even for small Cr doping amounts. On the other hand, Fe doping (from 3 to 7 at.%) reduces latent heat due to the reduction of the martensite cell distortion and leads to separation of martensitic and Curie transitions (reduces the martensitic transition temperature while does not significantly affect to the Curie temperature), improving the magnetization difference among both phases. This magnetization change increment together with the latent heat reduction reduces the magnetic field needed for driving completely the martensitic transformation. This effect also leads to higher isothermal entropy change values at moderate magnetic field changes of 1-2 T (30% enhancement) and to improve the sweeping rate of the martensitic transition with the magnetic field (which is directly related to the adiabatic temperature change). These features probe the applicability improvement for the Ni(Co)-Mn(Fe)-Ti alloys.

[1] Vinicius G. de Paula, Mario S. Reis, *Chemistry of Materials* **33**(14), 5483 (2021).

[2] A. Taubel *et al.*, *Acta Materialia* **201**, 425 (2020).

Acknowledgements: Work supported by AEI/FEDER-UE, Spain (grant PID2019-105720RB-I00), US/JUNTA/FEDER-UE, Spain (grant US-1260179), Consejería de Economía, Conocimiento, Empresas y Universidad de la Junta de Andalucía, Spain (grant P18-RT-746) and Sevilla University under VI PPIT-US program. Aun N. Khan acknowledges a FPI fellowship from the Spanish MICINN. LMMR acknowledges a postdoctoral fellowship from Junta de Andalucía and European Social Fund (ESF).

Magnetic nanostructures with different spin textures and topological protection

A. Parente^{1,*}, M. Abuin², José. L. Prieto², M. Menghini³, E. M. González^{1,3}, A. Muñoz-Noval^{1,3}

¹*Departamento de Física de Materiales, Facultad de Ciencias Físicas, Universidad Complutense, 28040 Madrid, Spain.*

²*Instituto de Sistemas Optoelectrónicos y Microelectrónica, Universidad Politécnica, 28040 Madrid, Spain.*

³*IMDEA Nanociencia, Cantoblanco, 28049 Madrid, Spain.*

*e-mail: aparente@ucm.es

New emergent phenomena due to topological effects have become a very active research frontier in condensed matter physics. Artificial magnetic nanostructures have opened a way to study topological phenomena such as frustration, emergent magnetic monopoles, synthetic antiferromagnetism or magnetic phase transitions.

In this work, different magnetic nanostructures with topological protection have been fabricated combining nanolithography techniques with DC magnetron sputtering. Morphological characterization using different microscopy techniques (AFM and SEM) and magnetic (magnetic force microscopy MFM) have been complemented with micromagnetic simulations in MuMax3 and transport measurements at low temperature.

The sensitivity of the textures and robustness of the topological protection in some of the structures under external magnetic fields have been investigated. The main goal of this work is to study the magnetic properties, spin textures and frustration in systems with different geometry and the influence of the geometry in the formation and ordering of magnetic defects.

Spin-orbit mixed states in an electromagnetic field

A. S. Miñarro*, Gervasi Herranz

Institut de Ciència de Materials de Barcelona (ICMAB-CSIC), Campus UAB, 08193 Bellaterra, Catalonia, Spain.

*e-mail: asanchez3@icmab.es

Spin-orbit mixing is an important problem in condensed matter. For instance, spin-orbit entanglement in the t_{2g} manifold may play an important role in exotic phenomena, like quantum spin liquids in 4d and 5d systems. An interesting question is how these states interact with electromagnetic fields, which may hold potential to tune their properties and reveal interesting physics. Motivated by our recent discovery of large gyrotropic signals in some Jahn-Teller manganites [1], here we explore the interaction of light with spin-mixed t_{2g} – e_g states in 3d metals. We show that spin-orbit mixing enables electronic transitions that are sensitive to circularly polarized light, giving rise to a gyrotropic response. Such interactions offer the opportunity to use electromagnetic waves at optical wavelengths to entangle orbital and spin degrees of freedom. Interestingly, we find that, in addition to spin-orbit coupling, orthorhombic Jahn-Teller interactions are relevant to enhance the observed optical gyrotropy in solid-state 3d systems with octahedral symmetry. Our approach, which includes a group-theoretic treatment of spin-orbit coupling, has wide applicability and provides a versatile tool to explore the interaction of electromagnetic fields with electronic states in transition metals with arbitrary spin-orbit coupling strength and point-group symmetries.

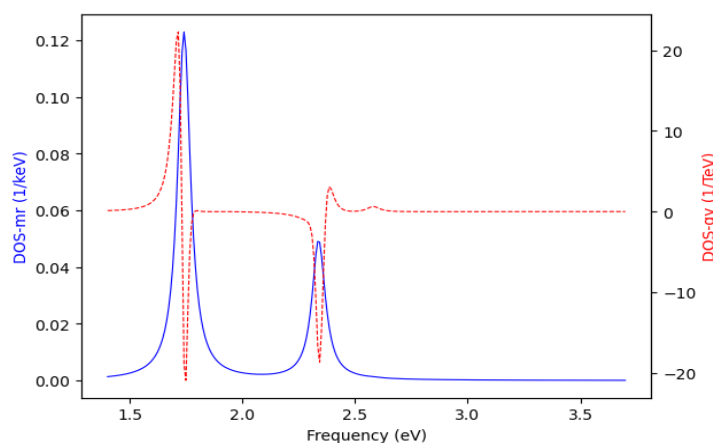


Figure 1. Non-gyrotropic (blue line) and gyrotropic (red line) signals taken from numerical calculations of the density of states of the non-perturbed ground states for the system perturbed with left-handed or right-handed circularly polarized light being the sum (left plus right) and the difference (left minus right) respectively.

[1] B. Casals et al., *Phys. Rev. Lett.* **117**, 026401 (2016).

Acknowledgements: This work is supported by the PID2020-118479RB-I00 and Severo Ochoa FUNFUTURE (CEX2019-000917-S) projects of the Spanish Ministry of Science and Innovation (MCIN/AEI/10.13039/501100011033).

Universal critical exponents of the magnetic domain wall depinning transition

Lucas Albornoz^{1,2,3}, Ezequiel Ferrero¹, Alejandro Kolton^{3,4}, Vincent Jeudy², **Sebastian Bustingorry**^{1,*}, Javier Curiale^{1,3}

¹*Instituto de Nanociencia y Nanotecnología, CNEA-CONICET, Centro Atómico Bariloche, (R8402AGP) S. C. de Bariloche, Río Negro, Argentina.* ²*Université Paris-Saclay, CNRS, Laboratoire de Physique des Solides, 91405 Orsay, France.* ³*Instituto Balseiro, Universidad Nacional de Cuyo-CNEA, Centro Atómico Bariloche, Avenida E. Bustillo 9500 (R8402AGP), San Carlos de Bariloche, Río Negro, Argentina.*

⁴*Centro Atómico Bariloche, Comisión Nacional de Energía Atómica (CNEA), Consejo Nacional de Investigaciones Científicas y Técnicas (CONICET), Avenida E. Bustillo 9500 (R8402AGP), San Carlos de Bariloche, Río Negro, Argentina.*

*e-mail: sbusting@cab.cnea.gov.ar

The depinning transition rules the low velocity response of domain walls in magnetic thin films. Understanding the depinning transition is key to unveil the role of disorder in magnetic systems. We present here results of magnetic-field-driven domain wall dynamics in a ferrimagnetic GdFeCo thin film with perpendicular magnetic anisotropy using low-temperature magneto-optical Kerr microscopy. Measurements performed in a practically athermal condition allow for the direct experimental determination of the velocity ($\beta = 0.30 \pm 0.03$) and correlation length ($\nu = 1.3 \pm 0.3$) exponents of the depinning transition [1]. The whole family of exponents characterizing the transition is deduced, providing evidence that the depinning of magnetic domain walls is better described by the quenched Edwards-Wilkinson universality class.

[1] L. A. Albornoz, E. E. Ferrero, A. B. Kolton, V. Jeudy, S. Bustingorry and J. Curiale, *Phys. Rev. B* **104**, L060404 (2021).

Acknowledgements: This work was supported by Grants No.PICT 2016-0069, No.PICT 2017-0906 and No.PICT 2017-1202 from the Agencia Nacional de Promoción Científica y Tecnológica, Argentina.

Novel magnetic nanostructures: nanopillars and patterned antidots

Elena Navarro¹, María Ujué González², Fanny Béron³, Felipe Tejo⁴, Juan Escrig⁵,
Andreas Kaidatzis⁶, Rafael P. del Real⁴, Raquel Álvaro², Dimitrios Niarchos⁶, Manuel Vázquez⁴,
José Miguel García-Martín^{2,*}

¹Dpto. de Física de Materiales, Universidad Complutense de Madrid, Madrid, Spain.

²Instituto de Micro y Nanotecnología, CSIC, Tres Cantos, Spain.

³Instituto de Física Gleb Wataghin, UNICAMP, Campinas, Brazil.

⁴Instituto de Ciencia de Materiales de Madrid, CSIC, Madrid, Spain.

⁵Departamento de Física, USACH, Santiago, Chile.

⁶Institute of Nanoscience and Nanotechnology, NCSR Demokritos, Athens, Greece.

*e-mail: josemiguel.garcia.martin@csic.es

Two different nanostructures are studied in this contribution: large-area nanopillar arrays fabricated by glancing angle deposition with magnetron sputtering (MS-GLAD) and magnetic thin films perforated with long-range order arrays of nanoholes prepared by focused ion beam (patterned antidots).

MS-GLAD is an easy and versatile route to fabricate arrays of nanostructures in large areas in a single processing step. In our work, nanostructured films with vertical or tilted nanopillars composed by polycrystalline Fe and Fe₂O₃ have been fabricated depending on whether the substrate is kept rotating azimuthally during deposition or not, respectively [1]. The magnetic properties of these films can be tuned with the specific morphology. In particular, the growth performed through a collimator mask mounted onto a not rotating azimuthally substrate produces almost isolated well-defined tilted nanopillars that exhibit a magnetic hardening. The first-order reversal curves diagrams and micromagnetic simulations revealed that a growth-induced uniaxial anisotropy, associated with an anisotropic surface morphology produced by the GLAD in the direction perpendicular to the atomic flux, plays an important role in the observed magnetic signatures.

Magnetic antidots are being studied for different applications, such as magnonic crystals for microwave devices, magnetically-active plasmonic media, magnetic biosensing, and magneto-resistance sensors. In our work, a top-down approach using focused ion beam has been employed to fabricate Co/Permalloy hard-soft bilayer antidot arrays [2]. The antidots have a 40 nm diameter and two symmetries are studied: square and hexagonal. A dependence of magnetic coercivity on the relative thicknesses of the magnetically hard (Co) and soft (Permalloy) layers is found; increasing Permalloy thickness results in lower magnetic coercivity. Furthermore, the long-range periodicity of these antidots results in higher magnetic coercivity and a stronger magnetic domain-wall pinning, compared to identical hard/soft bilayers of short-range order deposited on porous anodic alumina. Finally, magnetic force microscopy (MFM) imaging of the antidot arrays shows striking qualitative differences between the two symmetries: square symmetry arrays have inhomogeneous magnetic state and a high density of immobile super-domain walls, whereas hexagonal symmetry arrays show a homogeneous magnetic configuration.

[1] E. Navarro *et al.*, *Nanomaterials* **12**, 1186 (2022).

[2] A. Kaidatzis *et al.*, *J. Magn. Magn. Mat.* **498**, 166142 (2020).

Acknowledgements: The service from the MiNa Laboratory at IMN. Funding from MINECO, Comunidad de Madrid, European Union, Fondecyt, Dicyt-Usach, São Paulo Research Foundation, Brazilian National Council for S., NSRF Greece-EU, NATO.

Edge spin wave transmission through a vertex domain wall in triangular dots

Diego Caso^{1,*}, Farkhad Aliev^{1,2}

¹Departamento de Física de la Materia Condensada C03, Universidad Autónoma de Madrid, Cantoblanco, Madrid 28049, Spain. ²Instituto Nicolás Cabrera (INC) and Condensed Matter Physics Institute (IFIMAC), Universidad Autónoma de Madrid, Cantoblanco, Madrid 28049, Spain.

*e-mail: diego.caso@uam.es

Spin waves (SWs), being usually reflected by domain walls (DWs), could also be channeled along them. Recent studies allowed observation of spin waves along domain walls in rectangular, circular [1] and triangular dots in the ground or metastable states. Triangular dots could also present edge pinned inhomogeneous magnetic states, depending on the direction of the external magnetic field. These edge domain walls yield the interesting, and potentially applicable to real devices property of broadband spin wave confinement to the edges of the structure [2,3], with capabilities to be redirected at angles exceeding 100 degrees. It has been previously shown how these waves could be generalized for arbitrary shapes and propose few devices (such as edge spin wave interferometers, controllers or splitters) where edge spin waves could be implemented [3].

Here we present simulation results obtained on amorphous YIG ($Y_3Fe_5O_{12}$) based triangles where edge spin waves (ESW) were propagated over the corner in 2 micron sized triangles with a fixed thickness of 85 nm. The superior vertex angle, studied in the range of 40° - 75° , has been optimized in order to obtain a higher transmission coefficient over the vertex of the edge spin waves. Our simulations showed resonance increase of the ESW transmission for the angles close to 50 degrees. A slight excess of the transmission above one could be due to a positive interference with SWs propagating directly from the microwave field source to the opposite edge. A generated upper vertex domain wall's topology seems to be key in understanding the efficiency of the ESW propagation. We have investigated the phase shift of the SWs at the DW, which drops to $\pi/2$ at the high transmission range of angle apertures. We have also optimized the applied bias field to maximize the effectiveness of the exchange energy channels that behave as propagation routes for the spin wave.

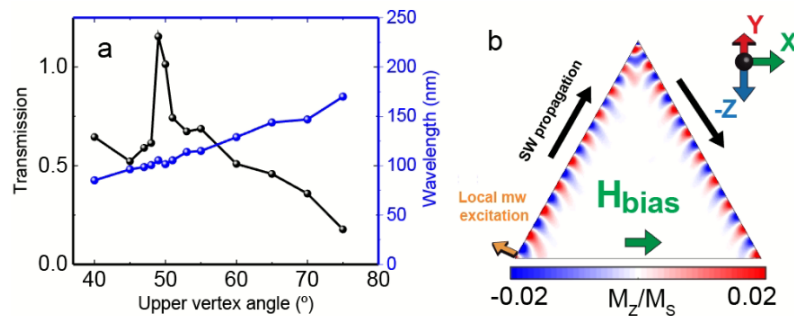


Figure 1. Wavelength of the signal and transmission coefficient of the ESW propagation through the upper vertex topology, showing a distinct increment for upper vertex angles in the 49-50 degree range. b) Snapshot of an edge spin wave propagated through both sides on a 2 micron side YIG triangle with a local microwave sinusoidal excitation perpendicular to the left side.

[1] F. G. Aliev, et al., *Phys. Rev. B* **84**, 144406 (2011).

[2] A. Lara, V. Metlushko, F. G. Aliev, *J. Appl. Phys.* **114**, 213905 (2013).

[3] A. Lara, J. Robledo, K.Y. Guslienko, F. G. Aliev, *Scientific Reports* **7**, 5597 (2017).

Acknowledgements: Authors acknowledge support by Spanish Ministerio de Ciencia (RTI2018-095303-B-C55, CEX2018-000805-M) and Consejería de Educación e Investigación de la Comunidad de Madrid (NANOMAGCOST-CM Ref. P2018/NMT-4321) Grants. D.C. has been supported by Comunidad de Madrid by contract through Consejería de Ciencia, Universidades e Investigación y Fondo Social Europeo (PEJ-2018-AI/IND-10364).

Synthesizing MnAlC / hydrogel composites for 3D-printing of alternative permanent magnets

Zaida Curbelo*, Ester M. Palmero, Cristina M. Montero, and Alberto Bollero
Group of Permanent Magnets and Applications, IMDEA Nanociencia, 28049 Madrid, Spain

*e-mail: zaida.curbelo@imdea.org

3D-printing technologies attract much interest in high-tech sectors due to the possibility of fabricating complex and high-performance objects with tailored properties and a minimal waste generation [1]. In the permanent magnets (PMs) sector, the manufacturing of magnets by 3D-printing requires a high filling factor and no deterioration of the magnetic properties. Many works on additive manufacturing (AM) of PMs focus on NdFeB, however the present challenge is finding alternative rare earth-free PMs to address the criticality of rare-earths. MnAl-based alloys are promising candidates thanks to its high availability and diminished environmental impact [2]. A recent technology known as Fused Filament Fabrication (FFF) [3] has proved the potential that MnAlC alloy shows to be used for the development of alternative PMs by AM.

This work is focused on developing magnetic composites, using a hydrogel as matrix material and gas-atomized MnAlC particles of ferromagnetic τ -phase were used as filler. Different amounts of MnAlC particles were considered to end with composites with several filler loading. The quasi-spherical MnAlC particles showed a mean particle size of 50 μm . Firstly, hydrogels were chemically synthesized using alginate (ALG) as precursor material, and methylcellulose (MC) that was incorporated as additive for thickening the resulting mixture [4]. Afterwards, the MnAlC particles were added and stirred for obtaining homogeneous composites. Different ALG:MC ratios were analysed (2.5:1 and 1:1), and it was found that 2.5:1 is a suitable proportion for AM as it allows an adequate viscosity of the resulting composite to be loaded in syringes (Fig. 1a) and used in the direct ink writing (DIW) 3D-printing technology.

Figures 1b and 1c show the Scanning Electron Microscopy (SEM) images of the resulting cured composites (PM particles / hydrogel), which manifest a smooth surface with the MnAlC particles well dispersed along the hydrogel matrix. The hysteresis loops of the cured composites with different MnAlC load were measured by Vibrating Sample Magnetometry (VSM). The magnetization curves in Fig. 1d reveal that the magnetization scales with the MnAlC content in the composite, while the coercive field remains constant. Magnetometry measurements show that the magnetic properties of the MnAlC particles are not deteriorated along the composite synthesis process. The synthesized composites based on MnAlC particles and hydrogel present suitable and promising properties for their application in the development of a new generation of alternative PMs by additive and bonding manufacturing technologies.

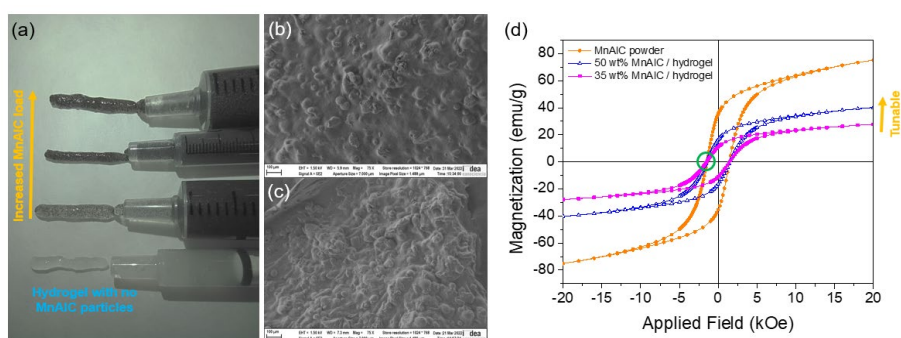


Figure 1. (a) Syringes loaded with hydrogel and composites with different MnAlC particles load; SEM images of the composites with (b) 35 wt% and (c) 50 wt% content of MnAlC particles [scale bar: 100 μm]; (d) Hysteresis loops for the composites with 35 wt% and 50 wt% MnAlC content, measured at room temperature.

- [1] L.E. Murr, *J. Mater. Sci. Technol.* **32**, 987 (2016).
 [2] J. Rial et al., *Acta Mater.* **157**, 42 (2018); C. Muñoz-Rodríguez et al., *J. Alloys Compd.* **847**, 156361 (2020).
 [3] E.M. Palmero et al., *Sci. Technol. Adv. Mater.* **19**, 465 (2018); *Addit. Manuf.* **33**, 101179 (2020).
 [4] D. Podstawczyk et al., *Addit. Manuf.* **34**, 101275 (2020).

Acknowledgements: Authors acknowledge Höganäs AB (Sweden) for providing the gas-atomized MnAlC particles through an industrial IMDEA-Höganäs collaboration and the financial support from MICINN by NEXUS (PID2020-115215RB-C21). E.M.P. acknowledges support from AEI through the Juan de la Cierva – Incorporación program (IJC2020-043011-I/MCIN/AEI/10.13039/501100011033) and EU by NextGenerationEU/PRTR.

Current- and Oersted-field- dynamics of a Bloch Point in cylindrical Ni nanowires

Jose A. Fernandez-Roldan^{1,2,*}, Cristina Bran²,
Manuel Vazquez², Oksana Chubykalo-Fesenko²

¹Department of physics, University of Oviedo, Oviedo, Spain. ²Helmholtz-Zentrum Dresden - Rossendorf e.V., Institute of Ion Beam Physics and Materials Research, 01328 Dresden, Germany.

³Instituto de Ciencia de Materiales de Madrid, ICM-CONIC, Madrid, Spain.

*e-mail: j.fernandez-rolan@hzdr.de

As three-dimensional nanomagnetism evolves, novel non-trivial magnetic textures emerge as appealing information carriers for spintronics based on curved nanosystems and particularly Cylindrical Nanowires (NWs) [1,2]. One of the most fascinating candidates that is likely to reach the high velocities required for fast recording technologies is the Bloch Point (BP) domain wall (DW). Recently, theoretical evidence indicated that BPs in NWs could reach high velocities close to 2 km/s in the magnonic regime [2]. While the observation of the BP DW in cylindrical NWs is no longer recent [2], scarce numerical studies that combine both spin-polarized current and Oersted field have been published in NWs [4,5], despite first attempts to measure DW velocities are in progress [6].

In this work we evaluate the dynamics of the BP DW under both current directions in a Ni NW with 100 nm in diameter. We investigate two cases: i) pre-nucleated BP DW, and ii) the BP DW formed from the transformation of a Vortex-Antivortex DW. Here the effects of both spin-polarized current and Oersted field are considered. We discuss in detail the role of the chirality of the BP in relation to the Oersted field, also reported previously in precursors of BPs [4].

Here we show that while the pre-nucleated DW with the same chirality as that of the Oersted field propagates always against the current direction, the BP originated either from the transformation of the BP with the opposite chirality or from the vortex-antivortex DW can either stop the propagation or propagate parallel to the current. Finally, we provide values of the velocities achieved by the BP in the NW as a function of applied current in Fig. 1.

We conclude that BPs with vanishing momentum propagate opposite to the current with velocities that may be suppressed by the Oersted field. Importantly for spintronic applications, momentum plays a major role in the dynamics of BPs that has not been envisaged up to know.

[1] A. Fernandez-Pacheco et al., Three-dimensional nanomagnetism. *Nat Commun* **8**, 15756 (2017).

[2] S. Da Col et al., Observation of Bloch-point domain walls in cylindrical magnetic nanowires, *Phys. Rev. B*, **89**, 180405 (2014).

[3] X.-P. Ma et al., Cherenkov-type three-dimensional breakdown behavior of the Bloch-point domain wall motion in the cylindrical nanowire, *Appl. Phys. Lett.* **117**, 062402 (2020).

[4] J.A. Fernandez-Roldan et al., Electric current and field control of vortex structures in cylindrical magnetic nanowires, *Phys. Rev. B* **102**, 024421 (2020).

[5] C. Bran et al, Magnetic Configurations in Modulated Cylindrical Nanowires, *Nanomaterials* **11**, 600 (2021). DOI: 10.3390/nano11030600

[6] M. Schöbitz et al., Fast Domain Wall Motion Governed by Topology and Oersted Fields in Cylindrical Magnetic Nanowires. *Phys. Rev. Lett.* **123**, 217201 (2019).

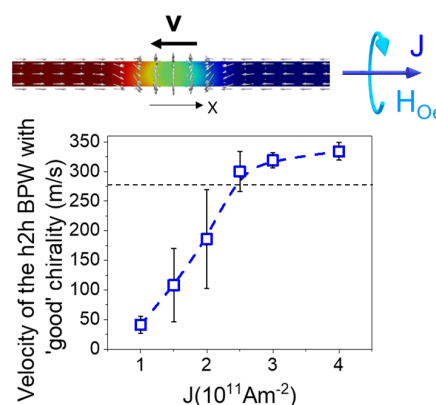


Figure 1. The mean velocity of a head-to-head Bloch Point DW driven by a spin-polarized current in a Ni nanowire as a function of the current density

Role of the particle size in the development of customized permanent magnet composites and flexible filaments for additive manufacturing

Ester M. Palmero*, Daniel Casalez, Javier de Vicente, and Alberto Bollero

Group of Permanent Magnets and Applications, IMDEA Nanociencia, 28049 Madrid, Spain

*e-mail: ester.palmero@imdea.org

Multi-material additive manufacturing (AM) is nowadays of large interest in high-technology sectors for fabricating complex high-performance objects with tailored properties [1]. For permanent magnets (PMs), the challenge is to develop magnets by AM with no geometrical restrictions, high loading (i.e., high filling factor, FF), and non-deteriorated PM properties [2], together with finding alternatives (e.g., improved ferrites and the promising MnAlC-based alloys) to rare earth-based magnets [3].

Highly loaded composites (PM particles/polymer) were synthesized by solution casting, followed by extrusion of filaments for 3D-printing by Fused Filament Fabrication (FFF) technology, being reported recently for the very first time (Fig. 1a) [4]. Several alternative PM materials were studied (gas-atomized τ -MnAlC, Sr-ferrite and hybrids -Sr-ferrite/NdFeB). Particle size and fine-to-coarse particles ratio (FP/CP) play a key role on the flexibility and powder loading of MnAlC filaments (length > 10 m), reaching FF > 80% and non-deteriorated PMs properties [4]. These results will be compared to the obtained for filaments based on Sr-ferrite (coercivity, $H_c \sim 3$ kOe, FF = 92%), NdFeB ($H_c = 10.2$ kOe, FF = 83%) and hybrid composites ($H_c = 8$ kOe, FF = 90%). MnAlC-based objects were 3D-printed under controlled temperature (Fig. 1a), proving, through magnetic flux density measurements, that alternative PM materials can be efficiently synthesized and processed to develop novel PMs by AM (Fig. 1b) [4].

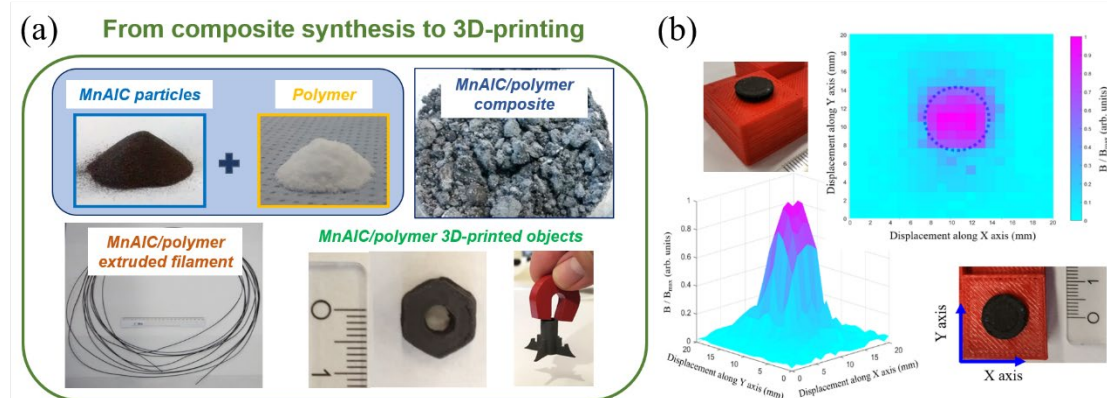


Figure 1. (a) Images of gas-atomized MnAlC particles, polymer, MnAlC/polymer composite, filament and 3D-printed objects; and (b) 3D-printed MnAlC-based disc together with the 3D plot and 2D maps of the magnetic flux density measured at the disc surface.

[1] L.E. Murr, *J. Mater. Sci. Technol.* **32**, 987 (2016).

[2] C. Huber et al., *Appl. Phys. Lett.* **109**, 162401 (2016); J. Jaćimović et al., *Adv. Eng. Mater.* **19**, 1700098 (2017).

[3] A. Bollero et al., *ACS Sustainable Chem. Eng.* **5**, 3243 (2017); J. Rial et al., *Acta Mater.* **157**, 42 (2018); J. Rial et al. *Engineering*, **6**, 173 (2020); C. Muñoz-Rodríguez et al., *J. Alloys Compd.* **847**, 156361 (2020).

[4] E.M. Palmero et al., *Sci. Technol. Adv. Mater.* **19**, 465 (2018); *IEEE Trans. Magn.* **55**, 2101004 (2019); *Addit. Manuf.* **33**, 101179 (2020).

Acknowledgements: Authors acknowledge collaborations with B. Skårman, H. Vidarsson and P.-O. Larsson (Höganäs, Sweden) by the industrial contract *GAMMA*, and A. Nieto and R. Altimira (IMA, Spain), and financial support from: MICINN by *NEXUS* project (PID2020-115215RB-C21); EU M-ERA.NET by *COSMAG* project (PCI2020-112143); and CM by *NanoMagCOST* project (P2018/NMT-4321). E.M.P. acknowledges support from AEI through the Juan de la Cierva – Incorporación program (IJC2020-043011-I/MCIN/AEI/10.13039/501100011033) and EU by NextGenerationEU/PRTR.

Electronic band structure of the Co pnictide $\text{Ca}(\text{CoAs})_2$ probed by ARPES

David Subires^{1,*}, L. Sánchez¹, J. Dai², M. Tallarida², T. Yilmaz³, E. Vescovo³,
M. Shatruk⁴, S. Blanco-Canosa^{1,5}

¹*Donostia International Physics Center (DIPC), E-20018 San Sebastián, Spain.*

²*ALBA Synchrotron Light Source, Cerdanyola del Vallès 08290, Catalonia, Spain.*

³*NSLS II, Brookhaven National Laboratory, Upton, New York, 11973, USA.*

⁴*Department of Chemistry and Biochemistry, Florida State University, Tallahassee, Florida 32306, USA.*

⁵*IKERBASQUE, Basque Foundation for Science, 48013 Bilbao, Spain.*

*e-mail: david.subires@dipc.org

Topological quantum materials represent an ideal scenario where to study the interplay between different interactions that can manifest interesting micro and macroscopic properties. One of this type of materials are the Weyl semimetals whose low-energy excitations are Weyl fermions. By the bulk-surface correspondence, these materials have topological protected Fermi arcs surface states. The experimental observation of these surface states gives an unequivocal proof that a particular compound is a Weyl semimetal [1]. Here, we report the experimental band structure of the recently predicted magnetic Weyl semimetal [2] Co-pnictide ACo_2X_2 ($A = \text{Ca}, \text{Ce}$ and $X = \text{P}, \text{As}$). We present the angle-resolved photoemission spectroscopy (ARPES) measurements and density functional theory calculations to describe the electronic band structure and the possible existence of Weyl fermions in $\text{Ca}(\text{CoAs})_2$.

[1] Su-Yang Xu et al., *Science*, **349**, 613-617 (2015).

[2] Yuanfeng, Xu et al., *Nature*, **586**, 702-707 (2020).

Temperature First Order Reversal Curves (TFORC) distributions of magnetocaloric materials

Luis M. Moreno-Ramírez*, Victorino Franco

Dpto. Física de la Materia Condensada, ICMS-CSIC Universidad de Sevilla, Spain.

*e-mail: lmoreno6@us.es

Magnetocaloric (MC) materials, those that experience a significant temperature change when submitted to magnetic field variations in adiabatic conditions, deserve the attention of the magnetic research community due to their implementation on a new energy efficient solid-state cooling technology. The effect is associated to significant magnetization changes driven by temperature and magnetic field, classifying the MC materials according to the order of their thermomagnetic phase transition: first- and second-order type. Typically, the materials undergoing first-order transitions present higher MC response than those with second order ones, although they have associated undesired thermal and magnetic hysteresis, which significantly reduce their response in cyclic conditions, limiting their applicability in refrigeration devices. Therefore, the understanding of the different sources and mechanism of hysteresis is a relevant topic in current research.

First Order Reversal Curve (FORC) distributions of magnetic materials is a well-recognized tool to extract information about magnetic interactions or to fingerprint magnetic materials. Recently, the possibility to use this technique to analyze the thermal hysteresis associated to the first-order magnetocaloric materials has been shown [1]. This so called TFORC technique is based on the analysis of the minor loops of the magnetization (M) in the hysteretic region, defining a certain set of reversal curves. These distributions represent the content of hysterons, which are defined as the elemental thermal hysteresis loop.

In this work, we set the basis for the interpretation of TFORC diagrams by performing a systematic study based on modelling of first-order phase transitions using a phenomenological transformation mechanism and correlating the obtained diagrams with the characteristics of the transition. The use of skewed normal distributions for modelling the transformation process between different phases allows us to calculate reversal magnetization curves. The transformation characteristics explored are: transition temperatures, temperature ranges of the transformations, symmetry/asymmetry between cooling and heating processes and existence of secondary phases. Each of them produces different shapes in the distributions, such as circular, ellipsoidal, semicircular or triangular [2]. In addition, we systematically modified the different distribution parameters to analyze the influence on the reversible magnetocaloric response and to link it to the different obtained TFORC distributions. The simulated results are compared to those of experimental data for a NiMnIn alloy, which allow us to separate the effects on the TFORC distributions of the structural transformation and the temperature dependence of magnetization of the martensitic and austenitic phases [3].

[1] V. Franco et al., *IEEE Magnetics Letters* **7**, 6602904 (2016).

[2] L. M. Moreno-Ramírez et al., *Metals* **10**, 1039 (2020).

[3] Á. Díaz-García et al., *Journal of Alloys and Compounds* **867**, 159184 (2021).

Acknowledgements: Work supported by AEI/FEDER-UE, Spain (grant PID2019-105720RB-I00), US/JUNTA/FEDER-UE, Spain (grant US-1260179), Consejería de Economía, Conocimiento, Empresas y Universidad de la Junta de Andalucía, Spain (grant P18-RT-746) and Sevilla University under VI PPIT-US program. LMMR acknowledges a postdoctoral fellowship from Junta de Andalucía and European Social Fund (ESF).

Magnetic Force Microscopy for biomedical applications

Miriam Jaafar^{1,2*}, Agustina Asenjo³

¹*Departamento de Física de la Materia Condensada and Condensed Matter Physics Center (IFIMAC), Universidad Autónoma de Madrid, Avda. Francisco Tomás y Valiente 7, 28049 Madrid, Spain.*

²*Instituto Nicolás Cabrera, Universidad Autónoma de Madrid, Avda. Francisco Tomás y Valiente 7, 28049 Madrid, Spain.*

³*Instituto de Ciencia de Materiales de Madrid (ICMM), Consejo Superior de Investigaciones Científicas (CSIC), C/Sor Juana Inés de la Cruz, 3, 28049 Madrid, Spain.*

*e-mail: miriam.jaafar@uam.es

Atomic Force Microscopy (AFM) is a powerful technique in biophysics and nanomedicine since it allows imaging and manipulating nanostructures in physiological conditions on a single molecule level [1]. Magnetic Force Microscopy (MFM) [2] is an AFM-based technique where a nanometric magnetic probe is scanned in close proximity to a surface detecting the local magnetic fields gradients near it. MFM has been applied to the study of a variety of magnetic systems, including magnetic nanoparticles. Advantages of MFM include relatively high spatial resolution, simplicity in operation as well as sample preparation. However, artifacts in the magnetic images can have strong impact and need to be carefully verified for a correct interpretation of the results. In general, when imaging magnetic materials with MFM the most typical artifact is the crosstalk between the topography and the magnetic signal. In addition, in some cases electrostatic signal could be also misinterpreted as magnetic information. With MFM we detect the magnetic force gradient between the tip and sample. However, during MFM imaging the tip stray field (sample stray field) can modify the sample (tip moment) configuration. These reversible or irreversible changes can be significant if the sample (tip) is magnetically soft.

Despite the importance of studying magnetic nanostructures with biological applications in physiological conditions, the applicability of MFM to these systems was limited up to now because of the difficulty in developing MFM for detecting magnetic interactions in liquids [3]. This is a consequence of the higher damping forces acting on the cantilever when working in liquid environment, as compared to air, which results in a significant loss of sensitivity of the MFM signal.

In the work presented here, we will explore new ideas combining non-standard MFM operation modes such as Bimodal MFM [4] with the information obtained from the experimental dissipation of energy associated to tip-sample interactions [5,6]. In addition, we will analyse the influence of the chosen cantilever on the obtained MFM signal-to-noise ratio. We will demonstrate that further improvement on the performance can be gained [7] by using magnetic probes fabricated by Focused Electron Beam Induced Deposition (FEBID) growth onto specially designed cantilevers for liquid medium.

[1] Dufrière Y. F. et al., *Nature Nanotechnology* **12**, 295 (2017).

[2] Kazakova, O.; Puttock, R.; Barton, C.; Corte-León, H.; Jaafar, M.; Neu, V.; Asenjo, A., *J. Appl. Phys.* **125**, 060901 (2019).

[3] P. Ares, M. Jaafar, A. Gil, J. Gómez-Herrero and A. Asenjo, *Small* **11**(36), 4731 (2015).

[4] Gisbert, V.G.; Amo, C.A.; Jaafar, M.; Asenjo, A.; Garcia, R., *Nanoscale* **13**, 2026 (2021).

[5] Jaafar M. and Asenjo A., *Appl. Sci.* **11**(22), 10507 (2021).

[6] Jaafar, M.; Iglesias-Freire, Ó.; García-Mochales, P.; Sáenz, J.J.; Asenjo, A., *Nanoscale* **8**, 16989 (2016).

[7] Jaafar M. et al., *Nanoscale* **12**, 10090(2020).